Oxidation mechanisms of Cr-containing steels and Ni-base alloys at high-temperatures – Part I: The different role of alloy grain boundaries

V.B. Trindade*, U. Krupp, Ph. E.-G. Wagenhuber, and H.-J. Christ

It is essential for materials used at high-temperatures in corrosive atmosphere to maintain their specific properties, such as good creep resistance, long fatigue life and sufficient high-temperature corrosion resistance. Usually, the corrosion resistance results from the formation of a protective scale with very low porosity, good adherence, high mechanical and thermodynamic stability and slow growth rate. Standard engineering materials in power generation technology are low-Cr steels. However, steels with higher Cr content, e.g., austenitic steels, or Ni-base alloys are used for components applied to more severe service conditions, e.g., more aggressive atmospheres and higher temperatures. Three categories of alloys were investigated in this study. These materials were oxidised in laboratory air at temperatures of 550 °C in the case of low-alloy steels, 750 °C in the case of an austenitic steel (TP347) and up to 1000 °C in the case of the Ni-base superalloys Inconel 625 Si and Inconel 718. Emphasis was put on the role of grain size on the internal and external oxidation processes. For this purpose various grain sizes were established by means of recrystallization heat treatment. In the case of low-Cr steels, thermogravimetric measurements revealed a substantially higher mass gain for steels with smaller grain sizes. This observation was attributed to the role of alloy grain boundaries as short-circuit diffusion paths for inward oxygen transport. For the austenitic steel, the situation is the other way round. The scale formed on specimens with smaller grain size consists mainly of Cr_2O_3 with some $FeCr_2O_4$ at localized sites, while for specimens with larger grain size a non-protective Fe oxide scale is formed. This finding supports the idea that substrate grain boundaries accelerate the chromium supply to the oxide/alloy phase interface. Finally, in the Ni-base superalloys deep intergranular oxidation attack was observed, taking place preferentially along random high-angle grain boundaries.

1 Introduction

As a result of a combination of reasonable mechanical properties, efficient corrosion resistance at high temperatures and lower cost compared with other high temperature materials, the Cr-containing steels are mainly used as material for components in power plants such as superheaters and exhaust systems. The surfaces of these tubes are exposed to combustion (outer side) and steam (inner side) atmospheres at temperatures between 400 and 600 °C resulting in a time-dependent loss in the tube thickness due to the reaction between gas and metal. It is known that a minimum Cr content of approximately 20 wt.% [1] is needed to establish the formation of a protective, continuous Cr_2O_3 scale on Fe-Cr alloys, which prevents further attack. For steels with lower Cr contents, complex oxide scales composed of hematite (Fe_2O_3), magnetite (Fe_3O_4), spinel ($FeCr_2O_4$), wustite (FeO) and chromia (Cr_2O_3) are formed. In several studies it is assumed that oxides on low-alloy steels grow mainly by outward Fe diffusion [2–4], due to the very small lattice diffusion coefficient of O anions in iron oxides. On the other hand, it was reported [5–8] that inward oxide growth contributes substantially to the overall oxidation process in the temperature range between 500 and 600 °C and that the mechanism for inward oxide growth may be attributed to the fast oxygen diffusion along oxide grain boundaries. Considering the relative high diffusivity along grain boundaries compared to that in bulk, the change in the substrate grain size should considerably influence the oxidation behaviour. Elsewhere [9, 10], the possibility of molecular oxygen permeation through micro-cracks and pores in the oxide scale was mentioned leading to inward oxidation.

The formation of a protective Cr_2O_3 scale is required to avoid degradation by severe corrosion processes for alloys used at high temperatures (up to 1000 °C). A number of investigations [11–15] were carried out to improve the understanding of the growth mechanism of Cr_2O_3 scales. The influence of oxide grain size as well as the effect of doping by rare earth elements, e.g., yttrium or cerium, on the growth kinetics of Cr_2O_3 were carefully investigated and even the diffusion coefficients of chromium and oxygen in the bulk and along grain boundaries of Cr_2O_3 are available [16, 17]. It is well established that Cr_2O_3 scales grow by counter-current diffusion of Cr and O [15, 18, 19].

In addition to the understanding of the mechanisms of Cr_2O_3 scale growth, it is important to know the minimum bulk concentration of Cr, which is necessary to form a protective scale on the entire surface, in order to prevent oxidation of the base material, e.g., Fe or Ni. Investigations reported a minimum value of Cr in the range between 18 and 20 wt.% [10]. However, this concentration range may depend strongly on the diffusion properties of Cr in the alloy. As a consequence, the grain size of the alloy should play an important role for the supply of Cr to the alloy/oxide interface, since the diffusivity

* *V.B. Trindade, U. Krupp, Ph. E.-G. Wagenhuber, H.-J. Christ,* Universität Siegen, Institut für Werkstofftechnik, Paul-Bonatz Str. 9-11, 57068-Siegen (Germany), E-mail: vicente@ifwt.mb.uni-siegen.de

 DOI: 10.1002/maco.200503879

of Cr along grain boundaries is much higher than that in the bulk [20].

Besides the formation of an external oxide scale, internal corrosion may occur under technical service conditions. In some cases, internal corrosion occurs preferentially along grain boundaries (intergranular corrosion). Of course, internal corrosion, particularly intergranular oxidation, is undesirable, since it usually enhances intergranular fracture resulting in premature brittle failure.

Depending on the alloy type (low-Cr steels, high-Cr steels or Ni-base alloys), the alloy grain boundaries play different roles on the oxidation behaviour. In this study emphasis was not only put on the kinetic aspects, but also on the thermodynamics of the oxidation processes in order to establish a mechanism-oriented model for oxidation of different alloys which is dealt with in part II of this paper.

2 Materials and experimental procedure

Three low-alloy ferritic steels ($c_{Cr} = 0.55-2.29$wt.%), one austenitic steel ($c_{Cr} = 17.5$wt.%) and two Ni-base alloys ($c_{Cr} = 18.2-19$wt.%) were used. The chemical compositions of these materials are given in Table 1.

The grain size was modified by applying a heat treatment at 1050 °C in inert gas atmosphere for 2, 12 and 112 h. The grain size was determined using optical microscopy in combination with the mean linear intercept technique. Fig. 1 illustrates the variation in grain size for the example of steel C.

The oxidation behaviour of the low-Cr steels and the austenitic steel was investigated for different grain sizes as summarized in Table 2. The Ni-base alloys were investigated only in the as-received condition.

Samples with dimensions $10 \times 10 \times 3$ mm^3 were used for thermogravimetric measurements. The samples were ground using SiC paper down to 1200 grid. They were finally cleaned ultrasonically in ethanol prior to oxidation. A hole of 1 mm diameter serves for hanging the samples in the thermobalance by means of a quartz wire. Isothermal and thermal-cycling thermogravimetric measurements were carried out using a SARTORIUS microbalance with a resolution of 10^{-6} g in combination with an alumina tube in a SiC furnace and an electronically controlled gas flow system. The low-alloy steels were oxidized at 550 °C, TP347 at 750 °C and the Ni-base superalloys at 1000 °C. After oxidation, the specimens were embedded in epoxy and carefully polished using diamond paste down to 1 μm and cleaned ultrasonically in ethanol. Analysis of the oxide phases and thickness measurements of oxide layers were performed using scanning electron microscopy (SEM) in combination with energy-dispersive X-ray spectroscopy (EDS) and electron back-scattered diffractometry (EBSD). X-ray diffraction (XRD) was employed to analyse the oxidation reaction products.

Table. 1. Nominal chemical composition (in wt. %) of the materials studied

	C	Cr	Si	Mn	Al	Mo	Ti	Fe	Ni
Steel A	0.076	0.55	0.36	1.01	0.04	---	---	bal.	0.21
Steel B	0.06	1.43	0.22	0.59	0.04	---	---	bal.	0.04
Steel C	0.09	2.29	0.23	0.59	0.01	1.0	---	bal.	0.44
TP 347	0.04	17.50	0.29	1.84	---	---	---	bal.	10.7
Inconel 625 Si	0.01	19.00	1.20	0.07	0.24	8.9	0.28	2.80	bal.
Inconel 718	0.04	18.20	0.40	0.06	0.50	3.0	1.00	18.70	bal.

Table. 2. Alloy grain size (in μm) of the materials studied

	as-received	2 h / 1050 °C	12 h / 1050 °C	112 h / 1050 °C
Steel A	6	24	---	54
Steel B	10	30	60	100
Steel C	4	13	---	74
TP 347	4	11	---	65
Inconel 625	30	---	---	---
Inconel 718	70	---	---	---

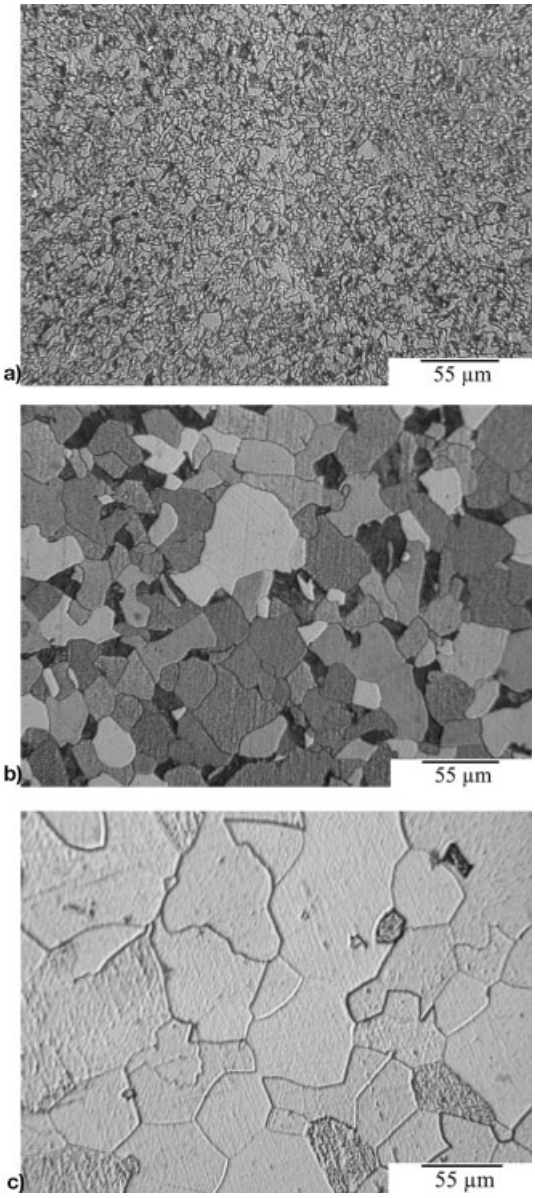

Fig. 1. Microstructure of the low-alloy steel C prior to oxidation with three different grain sizes: (a) 4 μm, (b) 13 μm, (c) 74 μm

3 Results and discussion

Kinetics of the oxidation process and related microstructural observations of the three classes of alloys are reported in separate sections in order to give a consistent description of the different role of the alloy grain size on the oxidation behaviour of these materials.

3.1 Low-alloy ferritic steels

The effect of the alloy grain size on the oxidation kinetics of low-Cr ferritic steels was carefully investigated using thermogravimetric measurements and confirmed by SEM observations. In all cases the oxide scale growth was nearly parabolic, i.e., kinetics can be described by means of a parabolic rate constant (k_p) and plotted against the alloy grain size. As shown in Fig. 2 the parabolic rate growth obviously decreases as the alloy grain size increases. Furthermore, the oxidation kinetics decreases as the Cr content increases for alloys with similar grain size.

By means of gold marker experiments it was possible to obtain a better understanding of the effect of alloy grain size on the oxidation mechanism. Prior to oxidation, a thin gold layer was sputter-deposited on the sample surface. After oxidation, the gold marker was found within the oxide scale (Fig. 3a), revealing two mechanisms of mass transport: (i) outward transport of Fe cations and (ii) inward transport of O anions. A detailed examination of the inner part of the scale revealed important features about the growth mechanism of the inner scale. By using different techniques (EDS mapping, XRD and EBSD) the oxide scale structure was characterized. The outer scale consists of Fe_2O_3 at the oxide/gas interface followed by Fe_3O_4. For the inner scale a more complex oxide structure was observed. Iror-chromium spinel ($FeCr_2O_4$) coexisting with Fe_3O_4 and some amount of Cr_2O_3 were identified. Thermodynamic calculations using the software FactSage (Fig. 3b) support these experimental observations.

The growth kinetics of the inner scale can be attributed to the high diffusivity of oxygen along alloy grain boundaries, supporting the experimental observations (Fig. 2 and Fig. 4). Fig. 4a documents clearly the effect of the alloy grain size on the thickness of the inner scale and compares this with the influence on the growth of the outer scale. As shown in Fig. 4b, preferential oxidation takes place along alloy grain boundaries and proceeds into the grain interior determining the progress of the inner scale/substrate interface.

3.2 High-alloy austenitic steel

Fig. 5 shows the thermogravimetrically measured mass gain of TP347 for different grain sizes during exposure at 750 °C to laboratory air. The sample with a grain size of 4 μm and 11 μm obeyed a parabolic rate law. At a grain size of 65 μm, oxidation kinetics is more complex and exhibits a stepwise parabolic behaviour, possibly due to the formation of a multilayer oxide scale and the occurrence of structural defects such as cracks and pores.

On top of the fine-grained specimens a very thin protective Cr_2O_3 scale was formed. However, locally the oxide scale was

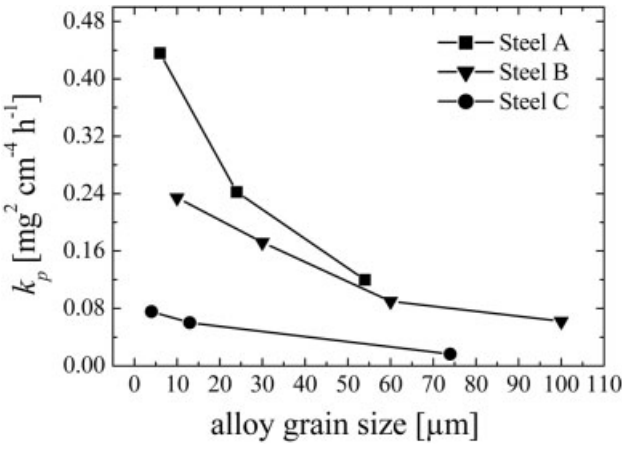

Fig. 2. Parabolic rate constant k_p of the three low-alloy steels oxidized in laboratory air at 550 °C for 72 h

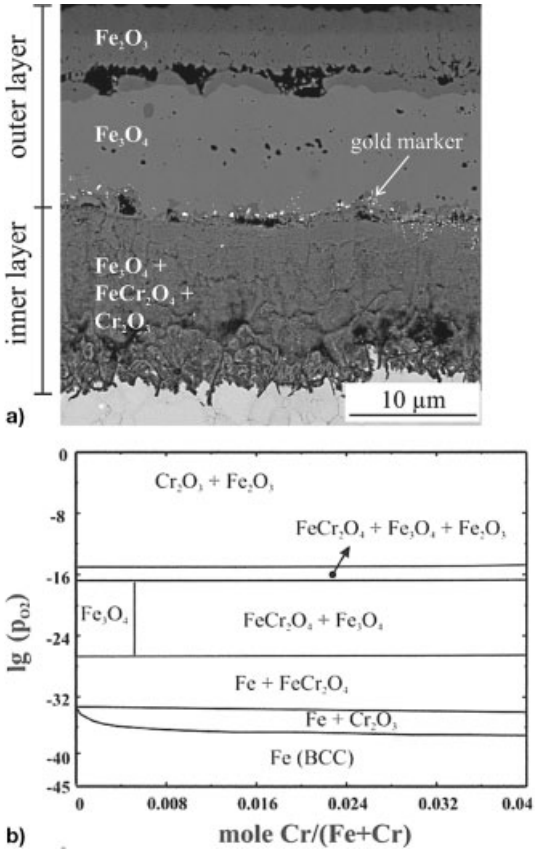

Fig. 3. (a) microstructural observations of the steel B oxidized in laboratory air at 550 °C for 72 h, (b) thermodynamic stability diagram of the system Fe-Cr-O calculated by means of the software FactSage

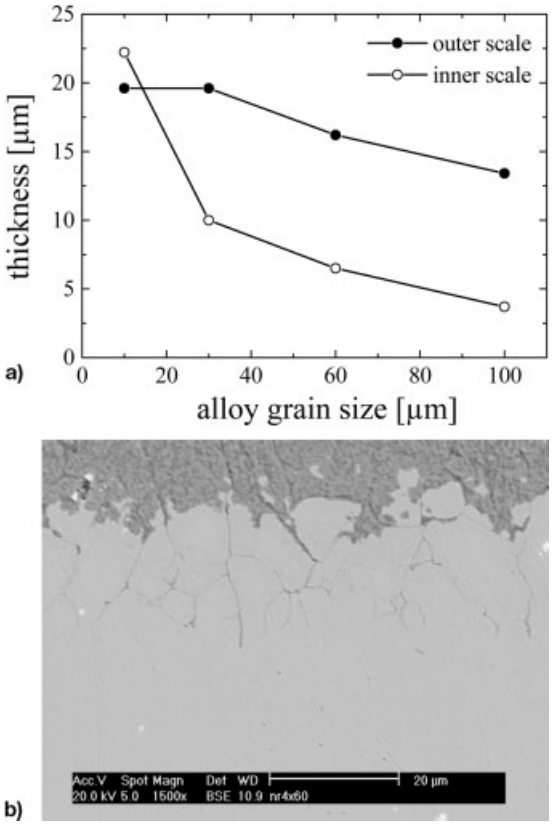

Fig. 4. (a) thickness of the inner and outer oxide scales formed on Steel B oxidized in laboratory air at 550 °C for a duration of 72 h and (b) intergranular oxidation along the inner scale/substrate interface

not totally protective leading to the formation of iron oxide nodules, which grow outward and inward. Generally, the formation of a protective Cr_2O_3 scale on specimens with a small grain size is favoured by a higher Cr flux from the bulk to the substrate/oxide interface as a consequence of the higher grain boundary density. On the coarse-grained specimen the oxide scale consists of an outer scale of iron oxide ($Fe_2O_3 + Fe_3O_4$) and an inner scale of mixed oxide phases containing Fe, Cr, Mn and Ni, similar to the oxide nodules formed on the fine-grained specimens. The distribution of the elements Cr and Fe (measured by EDS) is shown in Fig. 6.

Fig. 7 shows SEM micrographs of the surface oxide formed during the initial stage of the oxidation process on specimens with different grain sizes. A higher flux of Cr along the alloy grain boundaries leads to the formation of a thicker Cr_2O_3 scale on top of the grain boundaries as compared with the Cr_2O_3 scale formed on the interior of the grains (Fig. 7a) on specimens with small grain sizes. On the other hand, in the alloy with the large grain size of $d = 65\,\mu$m the flux of Cr towards the specimen surface is not sufficient in order to form a continuous and dense Cr_2O_3 scale and consequently to avoid fast oxidation of the base metal (Fe). Fig. 7b shows the formation of a thicker iron oxide in the interior of the grain and a thinner iron oxide enriched in Cr along the alloy grain boundaries.

From a thermodynamic point of view a rather low concentration of Cr is sufficient in order to form a Cr_2O_3 scale on Fe-Cr steels. However, the critical minimum concentration is much higher in reality, since the value of the Cr supply to the alloy/oxide interface must be taken into account. As shown in this study, the alloy grain size is an important factor to be considered. As a consequence of the high Cr diffusivity along alloy grain boundaries, fine-grained materials require a smaller Cr concentration than coarse-grained materials to form a slow-growing Cr_2O_3 scale on the entire surface.

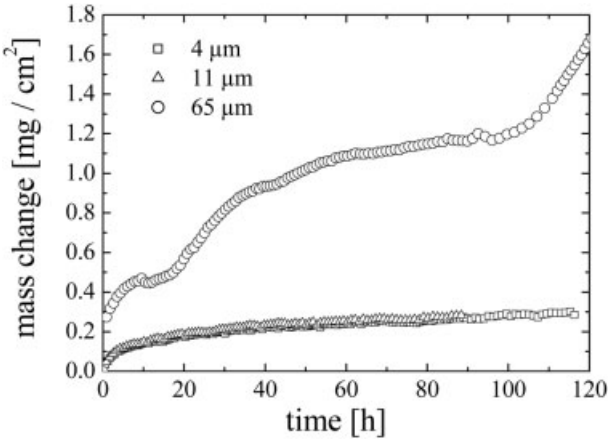

Fig. 5. Thermogravimetrically measured oxidation kinetics of TP347 with different grain sizes, for exposure at 750 °C to laboratory air for a duration of 120 h

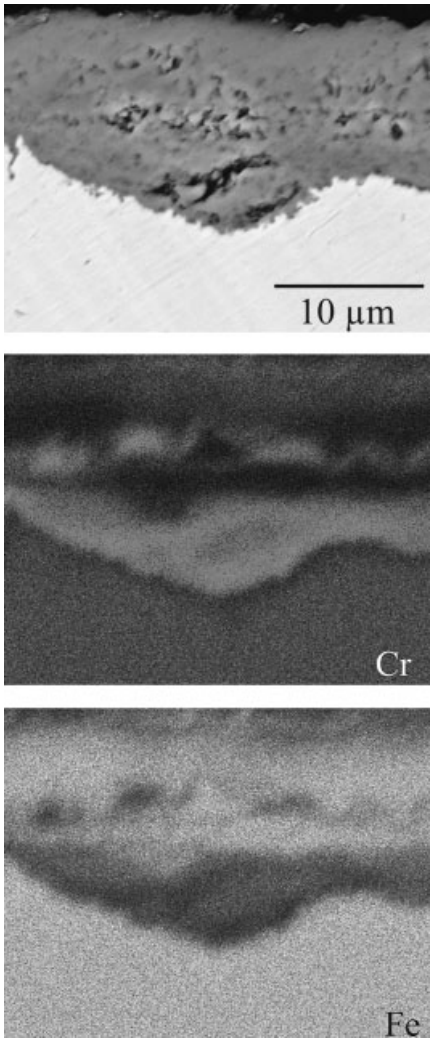

Fig. 6. Cross section and corresponding EDS element mappings (Fe, Cr) of the oxide scale formed on TP347 with a grain size of 65 μm during exposure to laboratory air at 750 °C for 120 h

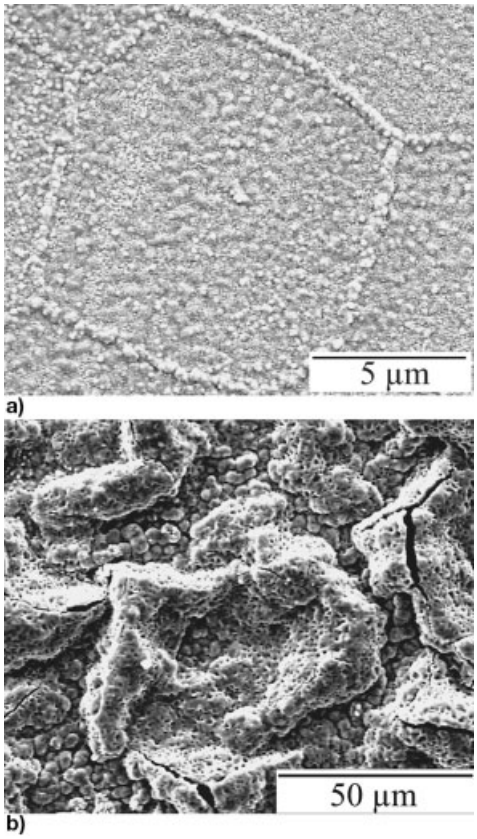

Fig. 7. Surface of the scale formed on TP347 at 750 °C after 1 h exposure to air: (a) formation of a thick Cr_2O_3 layer along grain boundaries on the fine-grained specimen (grain size = 11 μm) and (b) iron oxide formed on grain interior areas and Cr-enriched oxide formation along the grain boundaries of the coarse-grained specimen (grain size = 65 μm)

3.3 Ni-base alloys

The mass gain during isothermal exposure of the two studied Ni-base alloys (Inconel 625Si and Inconel 718) at 1000 °C followed the parabolic behaviour (Fig. 8). This observation is in agreement with the idea that for the both alloys the oxidation processes are controlled by solid state diffusion. The oxidation of Inconel 718 is substantially faster ($k_p = 0.374$ mg^{2}cm^{4}h^{-1}) than that of Inconel 625Si ($k_p = 0.0825$ mg^{2}cm$'^4$h^{-1}). Fig. 9 shows the oxide scales formed on the Ni-base alloys for the exposure to laboratory air at 1000 °C. A continuous external Cr_2O_3 oxide scale is formed on the surface of both alloys. In the case of Inconel 625Si, a discontinuous SiO_2 scale is formed underneath the Cr_2O_3 scale (Fig. 9a), which is probably responsible for the relatively low oxidation rate. Internal oxidation was observed in both alloys, occurring preferentially along alloy grain boundaries, enhanced by the fast oxygen diffusion along these short-circuit diffusion paths.

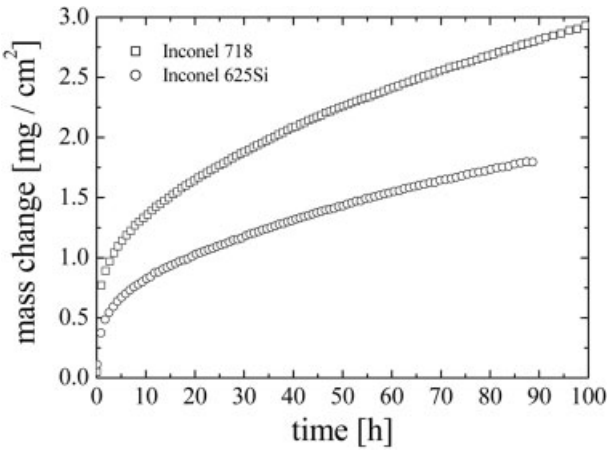

Fig. 8. Thermogravimetrically measured mass gain of Inconel 625Si and Inconel 718 for exposure to laboratory air at 1000 °C

4 Conclusions

This study revealed that oxide scales grow outward as well as inward at 550 °C in steels containing low Cr concentrations. An increased oxidation attack was observed with decreasing grain size due to higher oxygen transport along substrate grain boundaries.

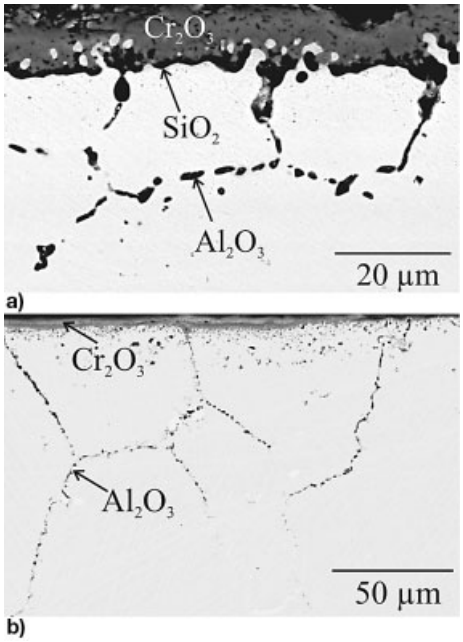

Fig. 9. Oxidation of Ni-base superalloys after exposure to laboratory air at 1000 °C: oxide scale and intergranular oxidation zone of (a) Inconel 625Si after 90 h and (b) Inconel 718 after 140 h exposure

A slow-growing Cr_2O_3 oxide was observed on high-alloy Cr steel (TP347) with small grain size due to the high density of grain boundaries leading to fast outward Cr transport along the substrate grain boundaries. Specimens with larger grain sizes form a complex mixture of Fe, Cr, Mn and Ni oxide. When adding Cr to high-temperature alloys in order to promote the formation of a slow-growing superficial Cr_2O_3, the high diffusivity of Cr along substrate grain boundaries must be considered. Grain boundary diffusion may significantly contribute to the Cr transport toward the substrate/oxide interface in materials with small grain sizes. Therefore, an alloy with a larger grain size requires a higher bulk Cr concentration to establish a protective Cr_2O_3 scale.

A significant intergranular attack consisting of a Al_2O_3 precipitation was observed for both Ni-base superalloys. Both alloys formed an outer Cr_2O_3 scale. In the case of Inconel 625Si a partial SiO_2 layer was formed underneath the Cr_2O_3 scale reducing its oxidation kinetics as compared with that of Inconel 718.

5 Acknowledgments

This research has been supported by the EU-project OPTICORR and by the Brazilian Research Foundation (CAPES) through a fellowship to one of the authors (*V.B. Trindade*).

6 References

[1] J. R. Davis, *Stainless Steels*, ASM Speciality Handbook, ASM, Materials Park, OH, **1994**.
[2] G. Granaud, R. A. Rapp, *Oxidation of Metals* **1977**, *11*, 193.
[3] J. E. Castle, P. L. Surman, *The Journal of Physical Chemistry* **1967**, *71*, 4255.
[4] L. Himmel, R. T. Mehl, C. E. Birchenall, *Journal of Metals* **1953**, *5*, 827.
[5] S. Matsunaga, T. Homma, *Oxidation of Metals* **1976**, *10*, 361.
[6] N. Appannagaari, S. Basu, *Journal of Applied Physic* **1995**, *78*, 2060.
[7] W. Wegener, G. Borchardt, *Oxidation of Metals* **1991**, *36*, 339.
[8] K. Nakagawa, Y. Matsunaga, T. Yanagisawa, *Materials at High Termperatures* **2001**, *18*, 51.
[9] R. Bredesen, P. Kofstad, *Oxidation of Metals* **1990**, *34*, 361.
[10] R. J. Hussey, M. Cohen, *Corrosion Science* **1971**, *11*, 713.
[11] R. C. Lobb, H. E. Evans, *Metal Science* **1981**, 267.
[12] D. R. Baer, M. D. Merz, *Metallurgical Transactions A* **1980**, *11A*, 1973.
[13] J. S. Dunning, D. E. Alman, J. C. Rawers, *Oxidation of Metals* **2002**, *57*, 409.
[14] F. J. Pérez, F. Pedraza, C. Sanz, M. P. Hierro, C. Gómez, *Materials and Corrosion* **2002**, *53*, 231.
[15] S. C. Tsai, A. M. Huntz, C. Dolin, *Materials Science and Engineering A* **1996**, *212*, 6.
[16] S. N. Basu, G. J. Yurek, *Oxidation of Metals* **1991**, *36*, 281.
[17] G. J. Yurek, D. Eisen, A. Garrat-Reed, *Metallurgical Transactions A* **1982**, *13A*, 473.
[18] A. M. Huntz, *Journal of Materials Science Letters* **1999**, *18*, 1981.
[19] A. F. Smith, *Metal Science* **1975**, *9*, 375.
[20] I. Kaur, W. Gust, *Fundamentals of Grain and Interphase Boundary Diffusion*, Ziegler Press, Stuttgart **1988**.

(Received: April 29, 2005) W 3879